International Journal of Engineering

Journal Homepage: www.ije.ir

Numerical Study on Vibration Attenuation of Cylinder using Active Rotary Oscillating Controller

A. H. Rabiee*

School of Mechanical Engineering, Arak University of Technology, Arak, Iran

P A P E R I N F O

Paper history:
Received 24 May 2019
Received in revised form 28 October 2020
Accepted 29 October 2020

Keywords:
Vortex-induced Vibration
Galloping
Square-section Cylinder
Active Rotary Oscillation

A B S T R A C T

The present article is an attempt at utilizing a feedback control system based on cylinder rotary oscillations in order to attenuate the two-degree-of-freedom vibrations of an elastically-supported square-section cylinder in presence of flow. The control system benefits from the cylinder rotational oscillations about its axis that acts according to lift coefficient feedback signal of the cylinder. Based on the performed numerical simulations, it becomes clear that the active control system has successfully mitigated the two-degree-of-freedom vibrations of square cylinder both in the lock-in region and galloping zone. For a Reynolds number of Re = 90 located in the lock-in region, the active rotary oscillating (ARO) controller has achieved a 98% reduction in the cylinder transverse vibration amplitude, while the corresponding value for the in-line vibration is 88%. Moreover, for a Reynolds number of Re = 250 in the galloping zone, the ARO controller has successfully attenuated the cylinder transverse vibration amplitude by 72%, while the same value for the in-line vibration is 70%. One also observes that the ARO controller decreases the amplitude of lift and drag coefficients in the lock-in region by, respectively, 95% and 94%. In contrast, the corresponding percentages for the cylinder in the galloping zone are 24% and 39%, respectively.

doi: *10.5829/ije.2021.34.01a.23*

1. INTRODUCTION

Fluid-solid interaction has been a subject of interest for engineers due its enormous importance in the design of marine risers and platforms, submarine transport pipelines, cooling systems in power plants especially nuclear plants, heat exchangers and suspending bridges [1-3]. Vortex-induced vibrations (VIV) are a subset of flow-induced vibrations (FIV) in which frequency synchronization between vortex shedding frequency and structural natural frequency generates high-amplitude self-excited vibrations. In addition to VIV, galloping is considered to be a type of FIV happening for cylinders of the non-circular cross section such as square cylinders [4, 5]. Galloping is defined as the self-excited instabilities that result in high-amplitude and low-frequency oscillations in Reynolds number ranges higher that VIV [6, 7]. In the galloping zone, the transverse motion of structure generates aerodynamic forces which in turn increase oscillations. Right after the flow velocity exceeds the critical value related to galloping, the vibration amplitude continuously rises with increasing flow velocity. High-amplitude vibrations related to VIV and galloping can bring about fatigue failure. Consequently, reduction of such instabilities using passive and active control strategies is of critical importance [8-10].

A plethora of passive methods have been utilized for FIV reduction. Passive methods are not dependent on external energy sources and are usually easier to implement compared with active control strategies [11, 12]. However, passive control methods are effective only in certain working conditions. In fact, to effectively reduce FIV, one needs to determine the physical properties of passive control systems beforehand. After that, changing these physical characteristics is either too difficult or impossible as the structural and environmental conditions would be changed. Active control approaches, unlike passive methods, alters the structure-flow system behavior by the direct application

*Corresponding Author Institutional Email: *rabiee@arakut.ac.ir* (A. H. Rabiee)

Please cite this article as: A. H. Rabiee, Numerical Study on Vibration Attenuation of Cylinder using Active Rotary Oscillating Controller, Transactions A: Basics Vol. 34, No. 01, (2021) 202-211

of energy to the system using actuators. Common examples of active control include acoustic excitation and rotating the cylinders, as well as suction and blowing [13-16]. Benefitting from constant rotation and/or oscillating rotation of cylinder is one of the most effective methods for controlling the oscillating forces exerted on a stationary cylinder as well as the vibration of an elastically-supported cylinder. This has been the center of attention of numerous researchers.

There have been several studies concerning flexibility mounted cylinders with cross-over vibrations; while relatively little research has been done on rotational oscillating or rotary cylinders. Dimotakis and Tokumaru [17] were probably the first researchers to investigate the open-loop strategy for flow behind an oscillating non-vibrating cylinder. They demonstrated that the strength of vortices could be severely decreased, along with noticeable suppression of drag coefficient. The drag suppression demonstrated by Dimotakis and Tokumaru [17] were confirmed by 2D flow calculations by He et al. [18]. Ray and Christofides [19] investigated the effect of a rotating control cylinder on the reduction of drag force exerted on a long cylinder using an open-loop control approach. Nazarinia et al. [20] investigated the flow around a cylinder subjected to forced translational and rotational oscillations, both numerically and experimentally, guiding them for a detailed understanding of flow control and wake structure. Lu et al. [21] used an active feedback control method to significantly suppress the lift force of a flow excited rotary oscillating circular cylinder. Leontini and Thompson [22] investigated externally applied rotary oscillations to control the flow behind a cylinder, which can only vibrate in the cross-over direction. They display that applied rotational oscillation can significantly increase the amplitude of cross-over vibration, which is beneficial for power generation. Du and Sun [23] used an active control approach in which applied torsional vibrations are used to suppress cross-over cylinder displacement. The FIV magnitudes in the "synchronization" region were significantly reduced by changing the vortex shedding frequency to the rotational oscillation frequency. Wong et al. [24] offered an experimental study of the dynamic behavior and vertical structure of a circular cylinder that rotates harmoniously and experiences flow-induced transverse vibrations. Hasheminejad et al. [13] adopted active control approach to reduce the 1D-VIV a circular cylinder at using external torsional vibrations.

Numerous methods have been proposed with regard to the reduction of vibrations caused by vortex-shedding of circular cylinders. On the contrary, few studies have been carried out on square-section cylinders. Owing to their sharp corners, these cylinders display a completely different behavior from circular cylinders [25, 26]. Minewitsch et al. [27] benefited from a finite element method (FEM) to study the interaction between the wake and streamwise oscillations of cylinders at Re = 200. Yang et al. [28] conducted numerical investigations based on FEM for rectangular-section cylinders oscillating in the cross-over direction. They found out that the vortex-shedding mechanisms of circular and rectangular cylinders are completely different. Singh et al. [29] considered the forced cross-over oscillations of square cylinders at different frequency ratios. Sen and Mittal [30] numerically evaluated the free vibration of a square cylinder able to oscillate in the transverse and streamwise directions in the Reynolds number range of 60–600. For a zero structural damping and a mass of ratio of 10, they noticed that the lock-in region starts from Re = 87, while galloping begins from Re = 175. Zhao et al. [31] studied the effect of flow-approaching angle on the two-degree-of-freedom (2-DoF) vibrations of a square cylinder with the mass ratio of 3 at Re = 100. In another study, Sen and Mittal [25] examined the 2-DoF vibrations of square cylinders for various mass ratios. They observed that the transverse vibrations of square cylinders in the galloping region increase at mass ratios higher than 5. Zhao [32] investigated the effect of aspect ratio, defined as the ratio of cylinder dimension in the transverse direction to the dimension in the streamwise direction, on the 1-DoF and 2-DoF vibrations of square and rectangular cylinders with a mass ratio of 10 at Re = 200.

A number of methods have been proposed with regard to the reduction of vibrations caused by vortex-shedding of circular cylinders. On the contrary, few studies have been carried out on square-section cylinders. Venkatraman and Narayanan [33] conducted a study on the active control of vibrations due to the vortex-shedding of a circular cylinder as well as the galloping of a square prism. They modeled the oscillating cylinder as a 1-DoF linear oscillator, on which the fluid effect was considered as an external disturbance. By applying a sinusoidal wave on piezoelectric ceramic actuators installed on a square cylinder, Cheng et al. [34] concurrently controlled the flow and structural vibrations. Dai et al. [35] investigated the effectiveness of time-delay control systems to reduce the high amplitude of an elastically-supported square cylinder. They demonstrated that time-delay controller can postpone the beginning of galloping vibrations. Using numerical simulations, Wu et al. [36] investigated the effect of twist angle on the vibration attenuation of a square cylinder that freely vibrated in the transverse direction. They showed that the twist of cylinder surface alters the separation point of vortex shedding which in turn changes the frequency of vortex shedding, hence the reduction in vibrations.

The above literature review shows that although extensive studies have been performed in the field of controlling the VIV of circular cylinders, few researches

have been conducted on the effect of employed techniques for square cylinders. Accordingly, this article considers the subject of active control of square cylinder based on the rotational oscillations of the cylinder as one of the best approaches for FIV mitigation that has successfully been applied for circular cylinders.

The rest of the article is as follows: section 2.1 presents the equations of flow and oscillator, followed by a summary of the solution technique of fluid-structure interaction in section 2.2. The mechanism of active rotary oscillating (ARO) controller is presented in section 2.3 and the validation of current study is delineated in section 2.4. In addition, section 3 demonstrates the results and discussions related to the ARO controller via several figures. Finally, the most important findings are outlined in section 4.

2. NUMERICAL APPROACH

2. 1. Equations of Flow and Oscillator The numerical analysis starts by utilizing the two-dimensional (2D) incompressible equations of Navier-Stokes (NS) for flow simulation which are concisely expressed as:

$$\frac{\partial \mathbf{u}}{\partial t} = -(\mathbf{u}.\nabla).\mathbf{u} - \nabla p + \frac{1}{\mathrm{Re}}\nabla^2\mathbf{u}, \qquad \nabla.\mathbf{u} = 0, \tag{1}$$

where $\mathbf{u}=(u_x/U, u_y/U)$ is the non-dimensional vector of flow velocity in which U represents the free flow velocity, p is the pressure, ρ is the density of fluid in question, and Re signifies the Reynolds number.

By submerging a rigid body in fluid, the vacillating torques and forces initiate the motion of body. In this article, the 2-DoF vibration of an elastically-supported rigid square-section cylinder is studied that is under the action of external rotary oscillations applied through the feedback control system. The schematic of problem is shown in Figure 1. Furthermore, the nondimensional 2-DoF motion equation developed for the cylinder is written as:

$$\frac{\partial^2 Q_i}{\partial t^2} + 4\pi\zeta\frac{\partial Q_i}{\partial t} + 4\pi^2 Q_i = \frac{V_r^2 C_i}{2m^*}, \tag{2}$$

where $Q_1 = X$ and $Q_2 = Y$ represent the nondimensional values of square cylinder motion amplitude along x and y directions, respectively. They are expressed as $Q_i = q_i / D$ in which q_i is the real displacement value and D signifies the side length of the studied cylinder. Also, $\zeta = c/\left(2\sqrt{km}\right)$ is the damping ratio quantity in which damping and stiffness coefficients are defined by c and k, respectively, $V_r = U / f_n D$ depicts the reduced speed

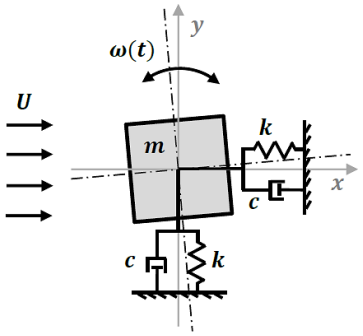

Figure 1. Schematic of flow-induced vibration on square-section cylinder

in which f_n is the structural natural frequency, $C_1 = C_D$ and $C_2 = C_L$. Finally, $m^* = m/m_d$ represents the mass ratio in which m and m_d are the mass of, respectively, cylinder and displaced fluid.

2. 2. Description of Fluid/Structure Solvers A brief introduction of the employed fluid/structure solvers and their most important properties are provided here. Aided by the computational fluid dynamics software package, ANSYS Fluent, along with a UDF otherwise known as user-defined function, Equation (1) is solved based on a time iteration approach. The computational domain of the cylinder is considered to be a rectangle. The distance between the cylinder center and the pair of domain upstream and downstream boundaries is shown by (L_u, L_d) as depicted in Figure 2. The dimension of the lateral boundary is displayed by H. In addition, the block ratio is defined as $B = D/H$. By considering a blockage ratio of 0.05, the finite volume mesh in question is displayed in Figure 3. The triangle meshes are deformed at each time step using the moving-deforming mesh function while the vibration and rotation of the cylinder inside the studied domain take place. The UDF written in C programming language decides what movement should be made in the central region. At the same time, unstructured meshes are rearranged in the external zone. The flow is considered as laminar unsteady for simulation purposes. An implicit pressure-based solver of first order is in charge of computing hydrodynamic loadings based on existing continuity and momentum relations. Other assumptions include non-slip boundary conditions on cylinder surface, free-stream velocity at the inflow, stress-free condition at the downstream boundary, zero cross-flow velocity and zero stress components on upper and lower boundaries. Furthermore, the UDF calculates the movement of the sprung cylinder according to the applied hydrodynamic forces. Fluent receives transverse and in-line velocities through the macro. In addition, surface boundary

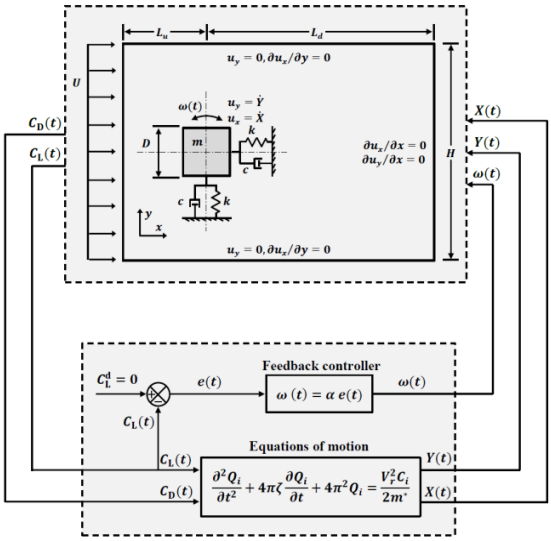

Figure 2. Block diagram of active rotary oscillating controller

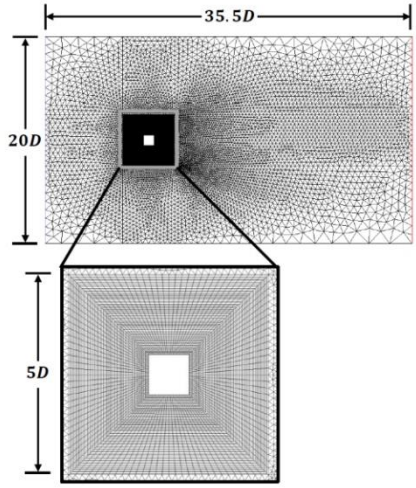

Figure 3. Utilized computational domain

condition $(\dot{x}_{n+1},\dot{y}_{n+1})=(u_x,u_y)$ is used to repeatedly determine various quantities including surface flow velocity, mesh arrangement and cylinder location. Refs. [37, 38] provide a more detailed explanation of flow-structure interaction.

2. 3. Active Rotary Oscillating Controller To restrain in-line and transverse movements in the current FIV arrangement, feedback control approaches are suitable choices in conjunction with the rotary oscillations of the cylinder. To this aim, one may choose the lift coefficient $C_{\mathrm{L}}(t)$ as the feedback signal from which the data on the flow-field close to the cylinder including the vortex shedding frequency are obtainable. Hence, the description of the proportional closed-loop controller can be written as:

$$\omega(t)=\alpha\, e(t), \tag{3}$$

where $\omega(t)$ represents the nondimensional angular velocity of the cylinder in question, $\alpha>0$ signifies the proportional gain of the controller. Also, $e(t)$ is described as:

$$e(t)=C_{\mathrm{L}}^{\mathrm{d}}(t)-C_{\mathrm{L}}(t), \tag{4}$$

where $C_{\mathrm{L}}^{\mathrm{d}}(t)$ is the desired quantity of lift coefficient. The present study assumes a zero value for $C_{\mathrm{L}}^{\mathrm{d}}(t)$, thus the control output is found to be:

$$\omega(t)=-\alpha\, C_{\mathrm{L}}(t). \tag{5}$$

One should note that he minus sign in Equation (5) shows that the direction of obtained lift coefficient $C_{\mathrm{L}}(t)$ is opposite to the imposed rotary oscillations $\omega(t)$. The overall arrangement of the control system is shown in Figure 2.

2. 4. Validation The input parameters for validating the performed numerical simulations are as follows: $m^*=10,\xi=0,B=0.05;F_N=f_N D/U \quad =14.39/\mathrm{Re}$. These values are used to obtain the changes in the peak amplitude of transverse oscillation for a 2-DoF sprung square-section cylinder with respect to different Reynolds numbers at a fixed blockage ratio of 0.05. As shown in Figure 4, a good agreement exists between the results of this study and those of Sen and Mittal [25], the latter of which is based on a special finite element analysis.

3. NUMERICAL RESULTS

To investigate the performance of ARO controller for the considered square cylinder with regard to the 2-DoF VIV and galloping, the parameters of the validation section are used [25]. In addition, the Reynolds numbers for the

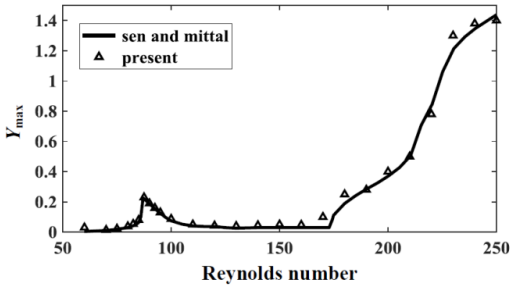

Figure 4. Variation of cylinder transverse displacement amplitude with Reynolds number

lock-in and galloping regions are taken as Re = 90 and Re = 250, respectively. For a blockage ratio of 0.05, the computational domain with $H = 20D$ is displayed in Figure 3 in which the center square section containing 7000 grid cells is located in a larger domain of 20000 grid cells.

First, the effect of control parameter value (α) on the transverse vibration amplitude of the square-section cylinder is investigated. For brevity, only the final results are reported here. The active rotary oscillating controller has a successful performance in the attenuation of cylinder transverse oscillations for a wide range of control parameters. As the control parameter increases, the maximum transverse displacement amplitude of cylinder first decreases and then rises. The maximum amount of reduction in cylinder transverse vibrations is achieved at Re = 90 with the control parameter $\alpha = 1.5$.

The time evolution response of the non-dimensional cross-flow and streamwise displacements of the cylinder for both controlled and uncontrolled cases can be seen in Figure 5 at the critical Reynolds number of 90 that is located in the lock-in region when the control parameter is $\alpha = 1.5$. One notices the sinusoidal response of cross-flow displacement whose frequency of oscillation is close to the vortex shedding frequency. On the other hand, the frequency of oscillation for the in-line displacement is twice as much. The ARO controller decreases the cross-flow vibration magnitude by up to 98%. The corresponding value for streamwise vibrations is 88%.

As discussed earlier, due to the different nature of galloping from VIV, it is good practice to separately study the effect of the active controller on the galloping of the square cylinder. A wide range of parameters are studied at Re = 250 in the galloping zone. It is noticed that $\alpha = 1$ yields the highest amount of reduction in the galloping of the square cylinder. The time evolution response of the non-dimensional cross-flow and streamwise displacements of the cylinder for both controlled and uncontrolled cases can be seen in Figure 6 at Re = 250 that is located in the galloping zone when the control parameter is $\alpha = 1$. The amount of reduction in cross-flow vibration by the active controller is 72%. The corresponding value for the attenuation of streamwise oscillation is 70%.

Comparing Figures 5 and 6 show that the uncontrolled response of the cylinder, especially for in-line oscillations in the galloping zone has significantly increased with respect to the lock-in region. Moreover, the amount of reduction in the vibration of the square cylinder in the lock-in region is more than the galloping zone. Next, to find the main reason behind the reduction of square cylinder vibrations by cylinder rotary oscillations in addition to the difference between the vibration reduction capability in the lock-in region and galloping zone, the values of force coefficients and vortex shedding frequency are inspected. The calculated values of controlled and uncontrolled lift and drag coefficients at Re = 90 (lock-in region) for $\alpha = 1.5$ as in the time evolution responses are shown in Figure 7. The computed magnitudes of lift and drag coefficients are decreased by as much as 95% and 94% using the ARO controller. This shows the capability of active rotary oscillating controller in decreasing the amplitude of lift and drag coefficients exerted on the square cylinder

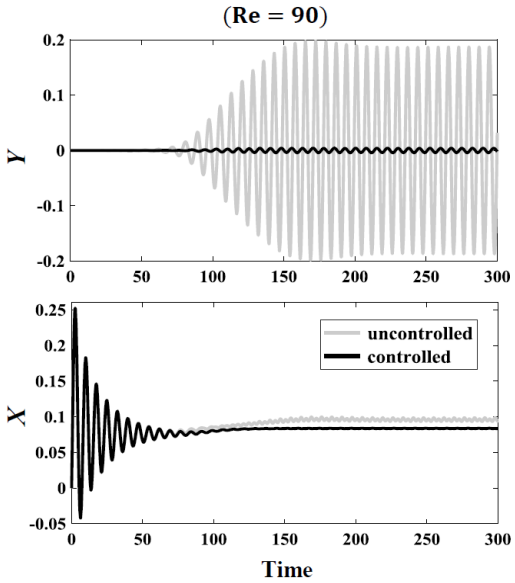

Figure 5. The time evolution of the non-dimensional cross-flow and streamwise displacements for controlled and uncontrolled cases at Re = 90

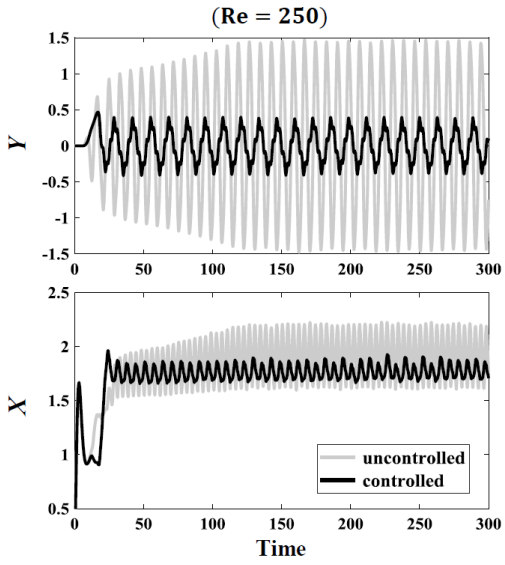

Figure 6. The time evolution of the non-dimensional cross-flow and streamwise displacements for controlled and uncontrolled cases at Re = 250

in the lock-in region. This in turn significantly reduces the transverse and in-line oscillations of the cylinder. The calculated values of controlled and uncontrolled lift and drag coefficient at Re = 250 (galloping zone) for $\alpha = 1$ as in the time evolution responses are shown in Figure 8.

The computed magnitudes of lift and drag coefficients are decreased by 24 and 39% using the ARO controller. As observed, the amount of reduction in the lift and drag coefficients of galloping zone are much less than the lock-in region. In addition, the regular and periodic oscillations of the controlled lift and drag coefficients related to the lock-in region have turned perturbatory. It is in fact concluded that the reduction mechanism of in-line and transverse vibrations for the lock-in region and galloping zone are different from each other.

For a more detailed evaluation, the power spectral densities corresponding to the active rotary oscillating controller as well as the uncontrolled cylinder are provided in Figure 9 for Re = 90 and Re = 250. The normalized vortex shedding frequency of the uncontrolled cylinder in this case ($f/f_n = 1$) at the Reynolds number of 90 is a sign of structural resonance, i.e. the vortex shedding frequency becomes equal to the natural frequency of structure. Using forced rotational oscillations of the cylinder, the feedback control system has successfully shifted down the normalized vortex shedding frequency from $f/f_n = 1$ to $f/f_n = 0.9$. Hence, frequency synchronization is disturbed and consequently, the energy transfer from flow to cylinder by the increase in the variations of lift coefficient has decreased significantly. These results in a reduction of cylinder transverse oscillations by 98%. On the other hand, at Re = 250 in the galloping zone, the normalized vortex shedding frequency is equal to $f/f_n = 0.87$. In this case, in which frequency synchronization has not occurred, the active controller has shifted down the vortex shedding frequency from $f/f_n = 0.87$ to $f/f_n = 0.55$.

Therefore, it is concluded that the main reason behind a reduction of 72% in the cross-flow oscillations of the cylinder in the galloping zone is the disturbance of surrounding flow and the weakening of flow-structure coupling and not the de-synchronization-type action. This explains why the reduction percentages of lift

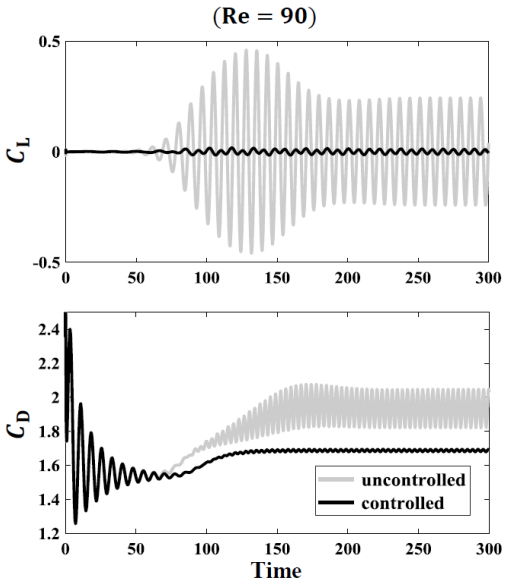

Figure 7. The time evolution of the lift and drag coefficients for controlled and uncontrolled cases at Re = 90

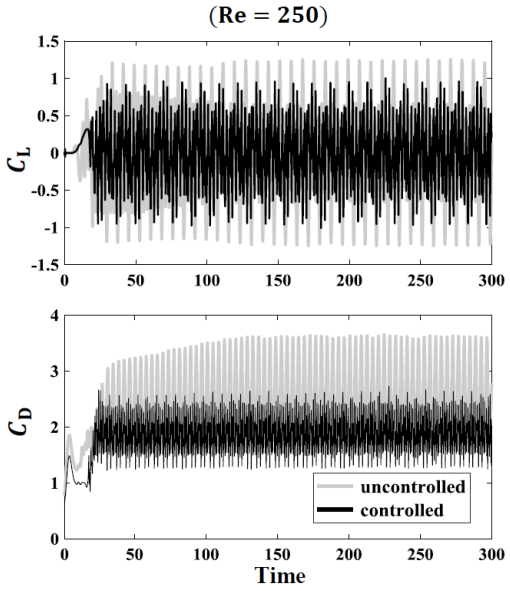

Figure 8. The time evolution of the lift and drag coefficients for controlled and uncontrolled cases at Re = 250

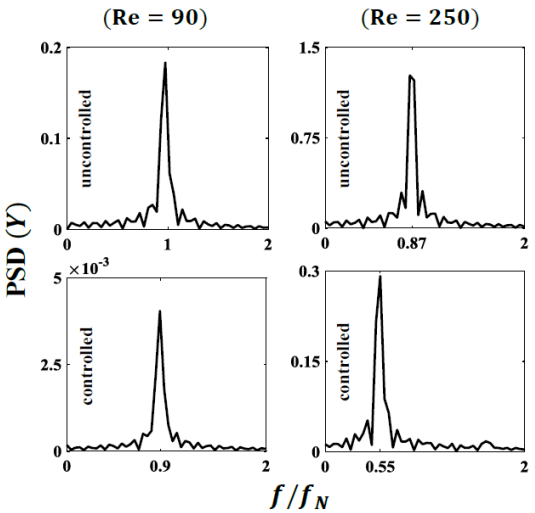

Figure 9. Power spectral density of cross-flow cylinder displacement for uncontrolled and controlled cases

coefficient and transverse vibrations of the cylinder are different in the lock-in region and galloping zone.

Figure 10 shows the time history of the relative error of controlled cylinders at Re = 90 and 250. As observed, the relative error in both the lock-in and galloping zones are small, although the performance of ARO controller in reducing the transverse oscillation of the cylinder in the lock-in region (Re = 90) is better than that in the galloping zone (Re = 250).

At this stage, to show the efficacy and robustness of ARO controller against possible structural uncertainties, the mass and stiffness of the cylinder are changed and numerical simulations are repeated with the same designed controller based on the nominal model. In this regard, Figures 11 and 12 show the time history of the transverse displacement of the square cylinder for ±20% variations in the cylinder mass and stiffness at Re = 90 and 250, respectively. As observed, the ARO controller, despite being developed according to the nominal model, has maintained its proper performance in spite of significant structural uncertainties.

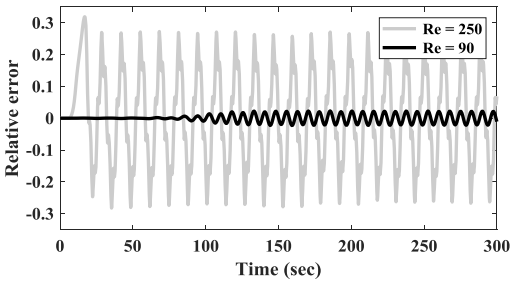

Figure 10. The time evolution of the relative error for controlled cases at Re = 90 and 250

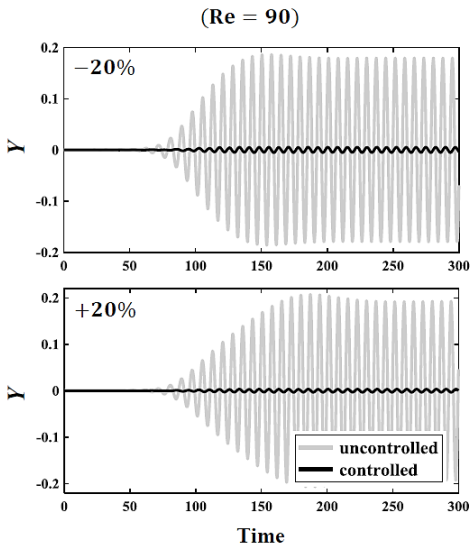

Figure 11. The robustenss of ARO controller with respect to ±20% perturbation in (m, k) at Re = 90

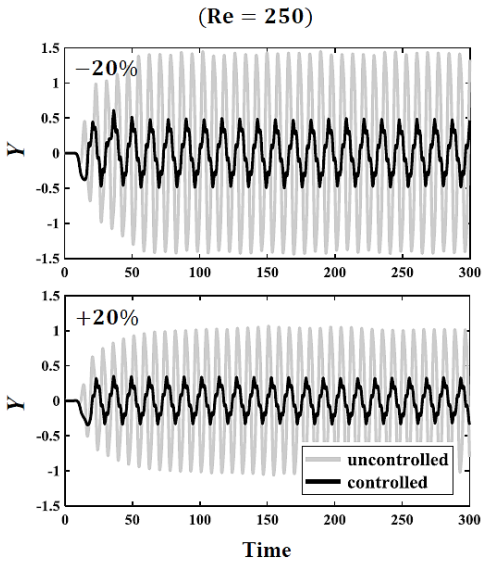

Figure 12. The robustenss of ARO controller with respect to ±20% perturbation in (m, k) at Re = 250

Finally, the correlations between the presented results are summarized as follows. The disturbance of frequency synchronization for the cylinder in the lock-in region reduces the lift coefficient, which in turn reduces the transverse oscillations of the cylinder. As a result, the main reason for the reduction of cylinder oscillations in the lock-in region is the disturbance of frequency synchronization. Regarding the cylinder in the galloping zone, the rotary oscillation disrupts the flow around the cylinder and weakens the fluid-structure coupling. This, and not the disturbance of frequency synchronization, is the main reason for the decrease in the transverse oscillations of the cylinder in the galloping zone. Reducing the lift coefficient as well as the transverse oscillations results in a relatively more smooth flow around the cylinder. Furthermore, as the equations of motion of the cylinder are coupled due to the flow, the drag coefficient on the cylinder also decreases. Accordingly, a decrease in streamwise oscillations owing to the reduction in the transverse oscillations of the cylinder can be observed in both the lock-in and galloping zones.

4. CONCLUSIONS

A closed-loop active control strategy was implemented to attenuate the two-degree-of-freedom vibrations of a square-section cylinder freely oscillating in the transverse and in-line directions in the lock-in and galloping regions. The control system benefited from the cylinder rotary oscillations about its axis which was based on the feedback signal from cylinder lift coefficient. Due to the difference between VIV and

galloping mechanisms, the effectiveness of control strategy was separately studied in both regions. VIV occurs when the vortex-shedding frequency equals the oscillator natural frequency. Galloping is specific to non-circular cylinders and causes high-amplitude, low-frequency oscillations in a range of Reynolds numbers greater than that of VIV. As soon as the flow velocity surpasses a critical value associated with galloping, the amplitude of vibrations continuously rises with increasing flow velocity. High-amplitude oscillations as a result of VIV and galloping can lead to catastrophic failures of structures. Thus, attenuating such instabilities is of utmost importance.

The main observations of the present study are discussed in what follows. The maximum percentage of reduction in cylinder transverse vibration was achieved in the lock-in region (Re = 90) for a control parameter value of $\alpha = 1.5$. At this Reynolds number, the ARO controller successfully reduced the amplitude of transverse and in-line vibrations of the cylinder by 98 and 88%, respectively. In addition, the reduction in the lift and drag coefficients in this region was equal to 95 and 94%, respectively. Moreover, the maximum amount of reduction percentage in cylinder transverse amplitude in the galloping zone (Re = 250) was realized using the control parameter $\alpha = 1$. At this Reynolds number, the ARO controller successfully decreased the amplitude of cylinder transverse vibration by 72%, while the corresponding value for the in-line vibration was 70%. Furthermore, the reduction in the lift and drag coefficients in this zone was, respectively, 24 and 39%. The normalized vortex shedding frequency for the uncontrolled square cylinder in the lock-in region was $f/f_n = 1$, indicating the synchronization of vortex shedding frequency with the natural frequency of structure. Here, the utilized control system successfully shifted down the vortex shedding frequency to $f/f_n = 0.9$. On the other hand, for a square cylinder in the galloping zone, the normalized vortex shedding frequency was equal to $f/f_n = 0.87$ that was further reduced to $f/f_n = 0.55$ with the aid of control system. Thus, it can be concluded that the main reason behind the reduction in the cylinder transverse vibration in the galloping zone is the disturbance of flow around the cylinder and weakening of structure-flow coupling and not the de-synchronization-type action. This describes the difference of lift coefficient and transverse vibrations of cylinder in the lock-in and galloping regions.

5. REFERENCES

1. Williamson, C., and Govardhan, R., "A brief review of recent results in vortex-induced vibrations", ***Journal of Wind Engineering and Industrial Aerodynamics***, Vol. 96, No. 6-7, (2008), 713-735. DOI: 10.1016/j.jweia.2007.06.019
2. Azizi, K., "Computational Fluid Dynamic-Two Fluid Model Study of Gas-Solid Heat Transfer in a Riser with Various Inclination Angles", ***International Journal of Engineering, Transaction A: Basics***, Vol. 30, No. 4, (2017), 464-472. DOI: 10.5829/idosi.ije.2017.30.04a.02
3. Rabiee, A. H., and Farahani, S. D., "Effect of synthetic jet on VIV and heat transfer behavior of heated sprung circular cylinder embedded in a channel", ***International Communications in Heat and Mass Transfer***, Vol. 119, (2020), 104977. DOI: 10.1016/j.icheatmasstransfer.2020.104977
4. Joly, A., Etienne, S., and Pelletier, D., "Galloping of square cylinders in cross-flow at low Reynolds numbers", ***Journal of Fluids and Structures***, Vol. 28, (2012), 232-243. DOI: 10.1016/j.jfluidstructs.2011.12.004
5. Sedaaghi, M. H., "Experimental investigation of the effect of splitter plate angle on the under-scouring of submarine pipeline due to steady current and clear water condition", ***International Journal of Engineering, Transactions C: Aspects***, Vol. 28, No. 3, (2015), 368-377. DOI: 10.5829/idosi.ije.2015.28.03c.05
6. Rabiee, A. H., "Galloping and VIV control of square-section cylinder utilizing direct opposing smart control force", ***Journal of Theoretical and Applied Vibration and Acoustics***, Vol. 5, No. 1, (2019), 69-84. DOI: 10.22064/TAVA.2019.113251.1144
7. Rabiee, A. H., and Farahani, S., "A comprehensive study of heat transfer characteristic and two-dimensional FIV for heated square-section cylinder with different damping ratios", ***International Communications in Heat and Mass Transfer***, Vol. 116, (2020), 104680. DOI: 10.1016/j.icheatmasstransfer.2020.104680
8. Rabiee, A. H., "Regenerative semi-active vortex-induced vibration control of elastic circular cylinder considering the effects of capacitance value and control parameters", ***Journal of Mechanical Science and Technology***, Vol. 32, No. 12, (2018), 5583-5595. DOI: 10.1007/s12206-018-1104-x
9. Rabiee, A. H., and Esmaeili, M., "Simultaneous vortex-and wake-induced vibration suppression of tandem-arranged circular cylinders using active feedback control system", ***Journal of Sound and Vibration***, Vol. 469, (2020), 115131. DOI: 10.1016/j.jsv.2019.115131
10. Hasheminejad, S. M., Rabiee, A. H., and Markazi, A., "Dual-Functional Electromagnetic Energy Harvesting and Vortex-Induced Vibration Control of an Elastically Mounted Circular Cylinder", ***Journal of Engineering Mechanics***, Vol. 144, No. 3, (2017), 04017184. DOI: 10.1061/(ASCE)EM.1943-7889.0001411
11. Kumar, R. A., Sohn, C.-H., and Gowda, B. H., "Passive control of vortex-induced vibrations: an overview", ***Recent Patents on Mechanical Engineering***, Vol. 1, No. 1, (2008), 1-11. DOI: 10.2174/1874477X10801010001
12. Golafshani, A., and Gholizad, A., "Passive vibration control for fatigue damage mitigation in steel jacket platforms", ***International Journal of Engineering, Transactions A: Basics***, Vol. 21, No. 4, (2008), 313-324.
13. Hasheminejad, S. M., Rabiee, A. H., and Bahrami, H., "Active closed-loop vortex-induced vibration control of an elastically mounted circular cylinder at low Reynolds number using feedback rotary oscillations", ***Acta Mechanica***, Vol. 229, No. 1, (2018), 231-250. DOI: 10.1007/s00707-017-1960-y
14. Muralidharan, K., Muddada, S., and Patnaik, B., "Numerical simulation of vortex induced vibrations and its control by suction and blowing", ***Applied Mathematical Modelling***, Vol. 37, No. 1-2, (2013), 284-307. DOI: 10.1016/j.apm.2012.02.028
15. Abbaspour, M., and Jahanmiri, M., "Experimental investigation of drag reduction on ahmed model using a combination of active flow control methods", ***International Journal of Engineering, Transactions A: Basics***, Vol. 24, No. 4, (2011), 403-410. DOI: 10.5829/idosi.ije.2011.24.04a.09

16. Rabiee, A. H., "Two-degree-of-freedom flow-induced vibration suppression of a circular cylinder via externally forced rotational oscillations: comparison of active open-loop and closed-loop control systems", ***Journal of the Brazilian Society of Mechanical Sciences and Engineering***, Vol. 42, No. 9, (2020), 1-15. DOI: 10.1007/s40430-020-02562-5

17. Dimotakis, P., and Tokumaru, P., Rotary oscillation control of a cylinder wake, Proceeding of 2nd Shear Flow Conference, 1-12, 1991.

18. He, J.-W., Glowinski, R., Metcalfe, R., Nordlander, A., and Periaux, J., "Active control and drag optimization for flow past a circular cylinder: I. Oscillatory cylinder rotation", ***Journal of Computational Physics***, Vol. 163, No. 1, (2000), 83-117. DOI: 10.1006/jcph.2000.6556

19. Ray, P., and Christofides, P. D., "Control of flow over a cylinder using rotational oscillations", ***Computers & Chemical Engineering***, Vol. 29, No. 4, (2005), 877-885. DOI: 10.1016/j.compchemeng.2004.09.014

20. Nazarinia, M., Jacono, D. L., Thompson, M. C., and Sheridan, J., "Flow over a cylinder subjected to combined translational and rotational oscillations", ***Journal of Fluids and Structures***, Vol. 32, (2012), 135-145. DOI: 10.1016/j.jfluidstructs.2011.05.005

21. Lu, L., Qin, J.-M., Teng, B., and Li, Y.-C., "Numerical investigations of lift suppression by feedback rotary oscillation of circular cylinder at low Reynolds number", ***Physics of Fluids***, Vol. 23, No. 3, (2011), 033601. DOI: 10.1063/1.3560379

22. Leontini, J., and Thompson, M., Active control of flow-induced vibration from bluff-body wakes: the response of an elastically-mounted cylinder to rotational forcing, Proceeding of 18th Australasian fluid mechanics conference, Launceston, Australia: Citeseer, pp. 1-4, 2012.

23. Du, L., and Sun, X., "Suppression of vortex-induced vibration using the rotary oscillation of a cylinder", ***Physics of Fluids***, Vol. 27, No. 2, (2015), 023603. DOI: 10.1063/1.4913353

24. Wong, K., Zhao, J., Jacono, D. L., Thompson, M., and Sheridan, J., "Experimental investigation of flow-induced vibration of a sinusoidally rotating circular cylinder", ***Journal of Fluid Mechanics***, Vol. 848, (2018), 430-466. DOI: 10.1017/jfm.2018.379

25. Sen, S., and Mittal, S., "Effect of mass ratio on free vibrations of a square cylinder at low Reynolds numbers", ***Journal of Fluids and Structures***, Vol. 54, (2015), 661-678. DOI: 10.1016/j.jfluidstructs.2015.01.006

26. Zhao, M., Cheng, L., and Zhou, T., "Numerical simulation of vortex-induced vibration of a square cylinder at a low Reynolds number", ***Physics of Fluids***, Vol. 25, No. 2, (2013), 023603. DOI: 10.1063/1.4792351

27. Minewitsch, S., Franke, R., and Rodi, W., "Numerical investigation of laminar vortex-shedding flow past a square cylinder oscillating in line with the mean flow", ***Journal of Fluids and Structures***, Vol. 8, No. 8, (1994), 787-802. DOI: 10.1016/S0889-9746(94)90280-1

28. Yang, S.-J., Chang, T.-R., and Fu, W.-S., "Numerical simulation of flow structures around an oscillating rectangular cylinder in a channel flow", ***Computational Mechanics***, Vol. 35, No. 5, (2005), 342-351. DOI: 10.1007/s00466-004-0621-x

29. Singh, A., De, A., Carpenter, V., Eswaran, V., and Muralidhar, K., "Flow past a transversely oscillating square cylinder in free stream at low Reynolds numbers", ***International Journal for Numerical Methods in Fluids***, Vol. 61, No. 6, (2009), 658-682. DOI: 10.1002/fld.1979

30. Sen, S., and Mittal, S., "Free vibration of a square cylinder at low Reynolds numbers", ***Journal of Fluids and Structures***, Vol. 27, No. 5, (2011), 875-884. DOI: 10.1016/j.jfluidstructs.2011.03.006

31. Zhao, J., Leontini, J. S., Jacono, D. L., and Sheridan, J., "Fluid–structure interaction of a square cylinder at different angles of attack", ***Journal of Fluid Mechanics***, Vol. 747, (2014), 688-721. DOI: 10.1017/jfm.2014.167

32. Zhao, M., "Flow-induced vibrations of square and rectangular cylinders at low Reynolds number", ***Fluid Dynamics Research***, Vol. 47, No. 2, (2015), 025502. DOI: 10.1088/0169-5983/47/2/025502

33. Venkatraman, K., and Narayanan, S., "Active control of flow-induced vibration", ***Journal of Sound and Vibration***, Vol. 162, No. 1, (1993), 43-55. DOI: 10.1006/jsvi.1993.1101

34. Cheng, L., Zhou, Y., and Zhang, M., "Perturbed interaction between vortex shedding and induced vibration", ***Journal of fluids and Structures***, Vol. 17, No. 7, (2003), 887-901. DOI: 10.1016/S0889-9746(03)00042-2

35. Dai, H., Abdelkefi, A., Wang, L., and Liu, W., "Control of cross-flow-induced vibrations of square cylinders using linear and nonlinear delayed feedbacks", ***Nonlinear Dynamics***, Vol. 78, No. 2, (2014), 907-919. DOI: 10.1007/s11071-014-1485-z

36. Wu, C.-H., Ma, S., Kang, C.-W., Lim, T.-B. A., Jaiman, R. K., Weymouth, G., and Tutty, O., "Suppression of vortex-induced vibration of a square cylinder via continuous twisting at moderate Reynolds numbers", ***Journal of Wind Engineering and Industrial Aerodynamics***, Vol. 177, (2018), 136-154. DOI: 10.1016/j.jweia.2018.03.030

37. Hasheminejad, S. M., Rabiee, A. H., Jarrahi, M., and Markazi, A., "Active vortex-induced vibration control of a circular cylinder at low Reynolds numbers using an adaptive fuzzy sliding mode controller", ***Journal of Fluids and Structures***, Vol. 50, (2014), 49-65. DOI: 10.1016/j.jfluidstructs.2014.06.011

38. Hasheminejad, S. M., Rabiee, A. H., and Jarrahi, M., "Semi-active vortex induced vibration control of an elastic elliptical cylinder with energy regeneration capability", ***International Journal of Structural Stability and Dynamics***, (2017), 1750107. DOI: 10.1142/S0219455417501073

Persian Abstract

چکیده

در این مقاله یک سیستم کنترل پس‌خور بر مبنای نوسانات چرخشی استوانه به منظور کاهش ارتعاشات دو درجه‌ی آزادی یک لوله با مقطع مربع در معرض جریان قرار گرفته بر روی بستر الاستیک به کار گرفته شده است. سیستم کنترل از نوسانات چرخشی استوانه حول محورش که بر مبنای فیدبک پس‌خور ضریب لیفت استوانه عمل می کند، بهره می‌گیرد. با توجه به شبیه سازی های عددی انجام شده مشخص می شود که سیستم کنترل فعال در کاهش نوسانات دو درجه آزادی استوانه مربعی هم در ناحیه‌ی قفل شدگی فرکانسی، و هم در ناحیه‌ی گالوپینگ موفق عمل کرده است. برای عدد رینولدز Re=90 واقع در ناحیه‌ی قفل شدگی فرکانسی، کنترلر فعال موفق شده است به مقدار ۹۸٪ دامنه ارتعاشات عرضی استوانه را کاهش دهد، در حالی که مقدار مشابه برای دامنه‌ی ارتعاشات طولی استوانه برابر با ۸۸٪ می‌باشد. همچنین برای عدد رینولدز Re=250 واقع در ناحیه‌ی گالوپینگ، کنترلر فعال موفق شده است دامنه‌ی ارتعاشات عرضی استوانه را به میزان ۷۲٪ کاهش دهد، در حالی که مقدار مشابه برای دامنه‌ی ارتعاشات طولی استوانه برابر با ۷۰٪ می‌باشد. همچنین، مشاهده می‌شود که کنترلر ARO موفق شده است دامنه‌ی ضرایب لیفت و درگ استوانه در ناحیه قفل شدگی را به ترتیب به میزان ۹۵ و ۹٤٪ کاهش دهد، درحالی که درصدهای مشابه برای استوانه در ناحیه‌ی گالوپینگ به ترتیب برابر با ۲٤ و ۳۹٪ می‌باشند